J|A|C|S
ARTICLES

Published on Web 07/20/2010

# Structural and Chemical Control in Assembly of Multicomponent Metal−Organic Coordination Networks on a Surface

Ziliang Shi and Nian Lin*

*Department of Physics, The Hong Kong University of Science and Technology, Clear Water Bay, Hong Kong, China*

Received March 5, 2010; E-mail: phnlin@ust.hk

***Abstract:*** Surface-supported supramolecular self-assembly has been used to generate multicomponent two-dimensional metal−organic coordination networks on a Au(111) surface. The networks consist of linker ligands of 4′,4‴-(1,4-phenylene)bis(2,2′:6′,2″-terpyridine) and nodal ligands of 5,10,15,20-tetra(4-pyridyl)porphyrin that are connected by pyridine−Fe−terpyridine motifs. Scanning tunneling microscopy revealed the coexistence of two polymorphic types of network structures (rhombus and Kagome). Through control of the dosage of the constituent ligands, homogeneous structural phases were obtained selectively. In particular, the rhombus structure could be converted into the more complex and more open Kagome structure by inclusion of guest molecules. Finally, coordination networks providing structural and chemical homogeneity were realized by judiciously choosing the dosages of the constituent ligands and the chemical substitution of the porphyrin ligands.

## Introduction

In the past few decades, supramolecular chemistry addressing intermolecular noncovalent interactions has attracted intensive attention.[1,2] In particular, metal−organic coordination interactions have been extensively explored in the reticular design of metal−organic framework (MOF) structures.[3−5] These structures represent a new class of materials that provide a wide range of applications, such as gas storage/separation, catalysis, and molecule-based magnets, as a result of their tunable structural and chemical characteristics.[6−10] Recently, multicomponent MOF structures have generated wide interest, as these structures are expected to exhibit multifunctional properties.[11,12]

Two-dimensional (2D) supramolecular coordination networks assembled directly at surfaces can be viewed as analogues of the three-dimensional (3D) MOFs. Although the assembly of surface-supported 2D coordination structures involves different chemistry than the solution-phase assembly of MOFs in 3D, the former has many characteristics similar to the latter. For example, it has been shown that rational design of the structure and chemistry could be achieved via a judicious choice of ligands.[13−15] As they are formed on solid substrates, the structures of these 2D networks and the self-assembly processes can be monitored in single-molecule detail using advanced surface science techniques, particularly scanning tunneling microscopy (STM).[13−15] For instance, STM revealed that self-recognition and self-selection play vital roles in controlling the self-assembly of two-component and even multicomponent systems.[16,17] Other examples include guest-molecule inclusion at the liquid−solid interface and template-assisted assembly on a metal surface, both illustrating how the relevant parameters guide the self-assembly at the single-molecule level.[18−20] These

(1) (a) Lehn, J.-M. *Science* **2002**, *295*, 2400. (b) Ikkala, O.; Brinke, G. T. *Science* **2002**, *295*, 2407. (c) Reinhoudt, D. N.; Crego-Calama, M. *Science* **2002**, *295*, 2403. (d) Hollingsworth, M. D. *Science* **2002**, *295*, 2410. (e) Hatzor, A.; Moav, T.; Cohen, H.; Matlis, S.; Libman, J.; Vaskevich, A.; Shanzer, A.; Rubinstein, I. *J. Am. Chem. Soc.* **1998**, *120*, 13469. (f) Yang, P.; Deng, T.; Zhao, D. Y.; Feng, P. Y.; Pine, D.; Chmelka, B. F.; Whitesides, G. M.; Stucky, G. D. *Science* **1998**, *282*, 2244.
(2) (a) Lehn, J.-M. *Eur. Rev.* **2009**, *17*, 263. (b) Lehn, J.-M. *Proc. Natl. Acad. Sci. U.S.A.* **2002**, *99*, 4763. (c) Lehn, J.-M. *Supramolecular Chemistry: Concepts and Perspectives*; VCH: Weinheim, Germany, 1995.
(3) Perry, J. J., IV; Perman, J. A.; Zaworotko, M. J. *Chem. Soc. Rev.* **2009**, *38*, 1400.
(4) Rosseinsky, M. J. *Microporous Mesoporous Mater.* **2004**, *73*, 15.
(5) Yaghi, O. M.; O'Keeffe, M.; Ockwig, N. W.; Chae, H. K.; Eddaoudi, M.; Kim, J. *Nature* **2003**, *423*, 705.
(6) Li, J.-R.; Kuppler, R. J.; Zhou, H.-C. *Chem. Soc. Rev.* **2009**, *38*, 1477.
(7) Murray, L. J.; Dincă, M.; Long, J. R. *Chem. Soc. Rev.* **2009**, *38*, 1294.
(8) Kurmoo, M. *Chem. Soc. Rev.* **2009**, *38*, 1353.
(9) Lee, J.; Farha, O. K.; Roberts, J.; Scheidt, K. A.; Nguyen, S. T.; Hupp, J. T. *Chem. Soc. Rev.* **2009**, *38*, 1450.
(10) Kitagawa, S.; Kitaura, R.; Noro, S. *Angew. Chem., Int. Ed.* **2004**, *43*, 2334.
(11) Maji, T. K.; Matsuda, R.; Kitagawa, S. *Nat. Mater.* **2007**, *6*, 142.
(12) Deng, H.; Doonan, C. J.; Furukawa, H.; Ferreira, R. B.; Towne, J.; Knobler, C. B.; Wang, B.; Yaghi, O. M. *Science* **2010**, *327*, 846.
(13) Lin, N.; Stepanow, S.; Ruben, M.; Barth, J. V. *Top. Curr. Chem.* **2009**, *287*, 1.
(14) Stepanow, S.; Lin, N.; Barth, J. V. *J. Phys: Condens. Matter* **2008**, *20*, 184002.
(15) (a) Bonifazi, D.; Mohnani, S.; Llanes-Pallas, A. *Chem.—Eur. J.* **2009**, *15*, 7004. (b) Kudernac, T.; Lei, S.; Elemans, J. A. A. W.; De Feyter, S. *Chem. Soc. Rev.* **2009**, *38*, 402. (c) De Feyter, S.; De Schryver, F. C. *J. Phys. Chem. B* **2005**, *109*, 4290.
(16) Langner, A.; Tait, S. L.; Lin, N.; Rajadurai, C.; Ruben, M.; Kern, K. *Proc. Natl. Acad. Sci. U.S.A.* **2007**, *104*, 17927.
(17) Llanes-Pallas, A.; Matena, M.; Jung, T.; Prato, M.; Stöhr, M.; Bonifazi, D. *Angew. Chem., Int. Ed.* **2008**, *47*, 7726.
(18) Lei, S.; Surin, M.; Tahara, K.; Adisoejoso, J.; Lazzaroni, R.; Tobe, Y.; De Feyter, S. *Nano Lett.* **2008**, *8*, 2541.


**10.1021/ja1018578** 

***Scheme 1.*** Chemical Structures and Molecular Dimensions of the Compounds Used in This Study: 4′,4‴′-(1,4-Phenylene)bis-(2,2′:6′,2″-terpyridine) (**1**), 5,10,15,20-Tetra(4-pyridyl)porphyrin (**2**), and Zinc 5,10,15,20-Tetra(4-pyridyl)porphyrin (**3**)

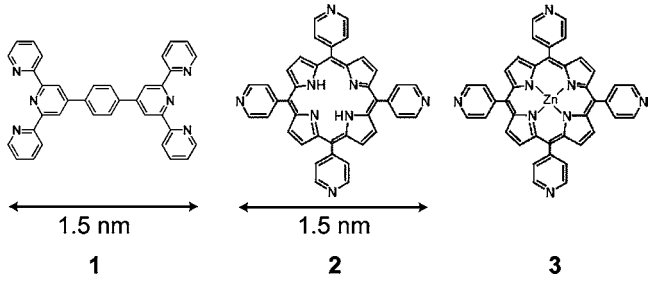


studies have provided unprecedented insights into various aspects of supramolecular self-assembly.

Here we report on the surface-supported self-assembly of multicomponent coordination networks with high structural complexity that exhibit two polymorphic phases (rhombus and Kagome). As the structural complexity advances, one of the central themes in synthesis is to control the chemical as well as structural characteristics accurately. For example, it is highly desirable to selectively form one structure out of many energy-equivalent (or closely equivalent) polymorphic phases. We demonstrate that through careful tuning of the relative and/or absolute dosages of the constituent molecular ligands, homogeneous network phases can be formed, in particular, via a guest−template mechanism. Our results highlight the important roles of guest molecules in the coordination self-assembly. Furthermore, a network structure of a homogeneous chemical state has been realized by chemical modification of the ligands.

## Experimental Section

In an ultrahigh-vacuum system (Omicron Nanotechnology), a single-crystalline Au(111) substrate was cleaned by cycles of Ar ion sputtering and annealing at ~900 K. The molecules **1**−**3** used in this study are shown in Scheme 1[21] (all were obtained from Aldrich, with purities of 96, 97, and 90%, respectively). At a base pressure of $<3 \times 10^{-10}$ mbar, molecules were evaporated by a molecular beam evaporator and deposited on the clean Au(111) surface, which was held at room temperature; the evaporation temperatures were 310 °C (compound **1**), 390 °C (compound **2**), and 410 °C (compound **3**). The molecular dosage was calibrated by analyzing STM data acquired from samples where molecules were clearly detectable. Iron atoms were evaporated from an iron rod (Goodfellow, 99.99%) by an electron-beam evaporator. The samples were annealed and transferred to an STM apparatus in vacuum. STM imaging was performed at room temperature in constant-current mode. To exclude any kinetic effects, we prepared the samples according to various evaporation sequences and annealing temperatures (180, 220, 260, or 310 °C). We confirmed that as long as the dosage of each component was fixed, the structures formed were independent of the preparation procedure.

## Results and Discussion

In the absence of Fe, molecules of **1** behave as a 2D molecular gas on the surface, whereas molecules of **2** and **3** form closely packed molecular adlayers on the surface.[22] Codeposition of **1** and **2** does not result in new phases. Only when molecules of **1**, **2** (or **3**), and Fe are codeposited on the surface do open-network structures appear. Figure 1a shows an overview STM topograph of the open-network structures formed by the self-assembly of **1**, **2**, and Fe. It is worthwhile to point out that **1** or **2** alone does not form open-network structures with Fe. Thus, we conclude that the open networks shown in Figure 1a are formed by a collective Fe coordinative bonding with the functional end groups of both **1** and **2**. Hence, the open-network structures represent 2D multicomponent metal−organic coordination networks.

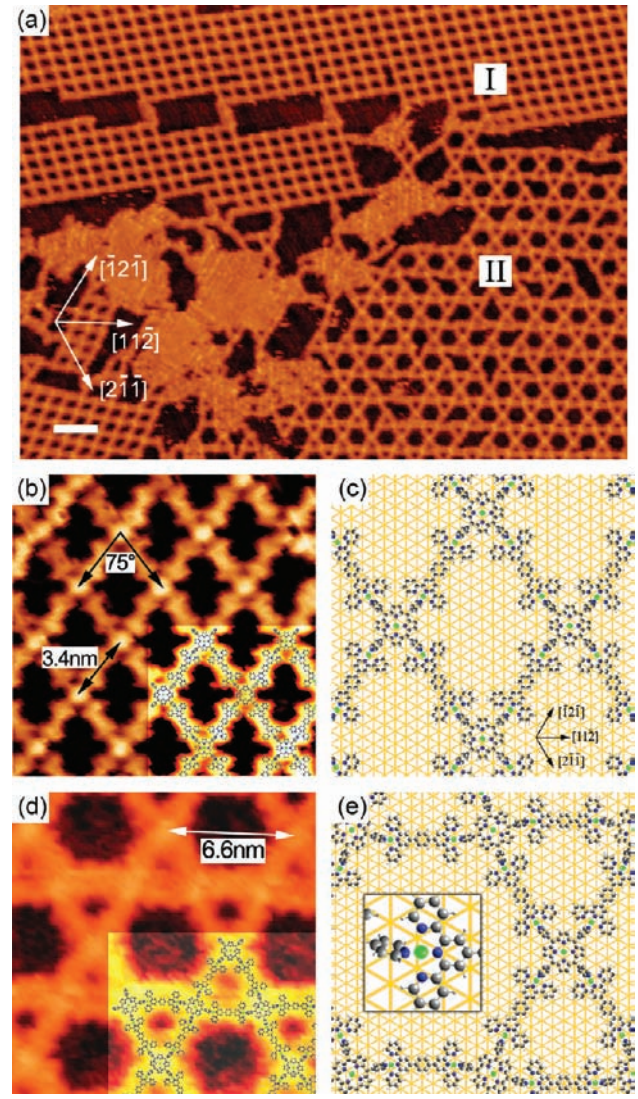


***Figure 1.*** (a) Overview STM topograph of the coexisting rhombic (type-I) and Kagome (type-II) phases (scale bar, 10 nm; data acquisition conditions: $U = 1.4$ V, $I = 0.4$ nA). (b, d) High-resolution images of the type-I and the type-II networks [size of each image, 15 nm × 15 nm; data acquisition conditions: (b) $U = -0.3$ V, $I = 0.3$ nA; (d) $U = -1.4$ V, $I = 0.5$ nA]. (c, e) Tentative models of the type-I and type-II networks on a Au(111) surface lattice. Inset in (e): close-up view of the fourfold-coordinated Fe center. Color code: C, gray; N, blue; Fe, green; H, white; Au (111) lattice, orange.

The two phases appearing in Figure 1a exhibit a rhombic structure (type I) and a Kagome structure (type II).[22,23] In the type-I structure, the side length of the rhombus is $3.4 \pm 0.1$ nm and the apex angle is $75 \pm 2°$. The networks of the type-I

(19) Kampschulte, L.; Lackinger, M.; Maier, A.-K.; Kishore, R. S. K.; Griessl, S.; Schmittel, M.; Heckl, W. M. *J. Phys. Chem. B* **2006**, *110*, 10829.
(20) Lin, N.; Langner, A.; Tait, S. L.; Rajadurai, C.; Ruben, M.; Kern, K. *Chem. Commun.* **2007**, 4860.
(21) Fleischer, E. B. *Inorg. Chem.* **1962**, *1*, 493.
(22) Shi, Z.; Lin, N. *ChemPhysChem* **2010**, *11*, 97.
(23) Shi, Z.; Lin, N. *J. Am. Chem. Soc.* **2009**, *131*, 5376.

structure follow three orientations with respect to the Au(111) surface lattice underneath (see Figure 1a). In the type-II structure, the side length of the Kagome hexagon is 3.3 ± 0.1 nm and the diameter of the hexagon is 6.6 ± 0.1 nm. This network structure exhibits a single orientation with respect to the Au(111) surface lattice in which the hexagonal diagonal directions lie along the $\langle 11\bar{2}\rangle$ directions. It is known that surface-supported 2D supramolecular structures are determined by intermolecular interactions as well as molecule-to-substrate interactions.[13,14] Here, the specific network orientations with respect to the substrate Au(111) lattice exemplify the role of molecule-to-substrate interactions.

In the high-resolution images (see Figure 1b), the molecules of **1** appear as a dog-bone shapes, manifesting the two terpyridyl end moieties. The STM data clearly reveal that the molecules of **1** act as network linkers while the molecules of **2** act as network nodes. Each molecule of **2** is attached to a molecule of **1** at each of its four terminals. Although Fe atoms were not resolved unambiguously in the STM topographs (which is a known phenomenon in 2D coordination systems[24,25]), we propose that it is the Fe center that links the pyridyl moiety of **2** with the terpyridyl moiety of **1**, as it is well-documented that Fe atoms or ions are able to coordinate pyridyl or terpyridyl moieties in bulk.[26,27] On the basis of the intrinsic molecular sizes of **1** and **2** (see Scheme 1) and the high-resolution STM data, we have constructed tentative models for the two network structures (Figure 1c,e; it should be noted that the porphyrin molecules are metalated in the models; we will discuss this issue in detail later). In both models, as illustrated in the inset of Figure 1e, the Fe center is coordinated by four nitrogen atoms, three from the terpyridine and one from the pyridine. To a first approximation, we assumed that the Fe atom is at the midpoint between the central nitrogen atom of the terpyridine and the pyridine nitrogen. In such a configuration, the Fe atom is shifted away from the Au(111) bridge site toward the hollow site by 0.3 Å. The distance between the two nitrogen atoms is ∼3.1 Å, leading to a distance of ∼1.6 Å between the Fe atom and each of the two N atoms, supposing that the Fe atom is in the same plane as the ligand molecules. The 1.6 Å Fe−N distance is shorter than the previously reported ones in bulk (1.9−2.2 Å).[28] However, a longer Fe−N bond is feasible if the Fe atom is out of the molecular plane. The other two nitrogen atoms of the terpyridine bind to the Fe center symmetrically with an Fe−N distance of 2.3 Å. Overall, the Fe center is fourfold-coordinated, which is rare in pyridyl or terpyridyl coordination in bulk. To date, various 2D coordination configurations that are different from the conventional 3D configurations, including two-, three-, and fourfold configurations, have been identified.[13,14] The terpyridine−Fe−pyridine coordination reported here represents a new 2D bonding motif that deserves further investigation of, for instance, its Fe oxidation state,[29] bond lengths, and bond angle.

In the models, the network structures are commensurate with the substrate Au(111) lattice (see Figure 1c,e). The molecules of **1** are adsorbed on the surface with their central phenyl rings sitting on the top sites and their long axes along the $\langle 11\bar{2}\rangle$ directions, while the molecules of **2** are adsorbed on the surface with their central macrocycles sitting on the bridge sites and their twofold-symmetry axes along the $\langle 11\bar{2}\rangle$ directions. Thus, the two types of networks exhibit similar molecular/atom adsorption configurations and similar coordination bonding configurations (e.g., coordination number, bond length, and bond angle). In addition, the two phases possess an identical **2**/**1**/Fe stoichiometry ratio of 1:2:4 (ignoring the metalation of the macrocycle of **2**). These similarities suggest that the formation energies of the two polymorphic structures are very similar, which presumably results in the coexistence of the two phases. The major difference lies in their network geometries: (1) The type-I structure consists of uniformly sized rhombic voids, but the type-II structure consists of larger hexagonal voids and smaller triangular voids. (2) The type-I structure has three orientations with respect to the Au(111) surface, but the type-II structure follows a single orientation. (3) The type-I structure occupies a slightly smaller unit surface area (10 $nm^2$ per molecule of **2**) than the type-II structure (12 $nm^2$ per molecule of **2**).

Next, we discuss how to selectively achieve a pure phase of either type-I or type-II by adjusting the self-assembly conditions. First, we found that when the surface is partially covered by the networks and the dosage of **1** is higher than its normal stoichiometry value, the pure type-I phase is formed. Figure 2a shows a representative STM topograph of this phase. One may note that the ribbonlike islands of the type-I structure are elongated along the $\langle 11\bar{2}\rangle$ directions of the Au(111) surface, implying that the growth of the isotropic islands is likely dictated by the Au(111) surface lattice. Careful examination (see the inset in Figure 2a) reveals that the short axis of the type-I rhombic lattice strictly follows the ridge direction of the $23 \times \sqrt{3}$ herringbone domain (indicated by the black lines) of the reconstructed Au(111) surface.[30] Obviously, extending the network islands across the herringbone domain boundaries would violate such a correlation, which is presumably unfavorable in terms of energy. Consequently, the growth of the network islands is confined within the two boundaries of a herringbone domain (indicated by the white lines), resulting in the anisotropic growth of the network islands. A similar templating effect of the Au(111) herringbone reconstruction was reported in the growth of molecular/atomic clusters/islands.[31] Here we have demonstrated that the assembly of coordination networks is also affected by the herringbone reconstruction.

When the overall molecular dosage is increased while the dosage of **1** is maintained at a value higher than its normal stoichiometry value, islands of the type-I phase cover the surface almost entirely, as shown by the representative STM topograph

(24) Tait, S. L.; Langner, A.; Lin, N.; Stepanow, S.; Rajadurai, C.; Ruben, M.; Kern, K. *J. Phys. Chem. C* **2007**, *111*, 10982.
(25) Classen, T.; Fratesi, G.; Costantini, G.; Fabris, S.; Stadler, F. L.; Kim, C.; De Gironcoli, S.; Baroni, S.; Kern, K. *Angew. Chem., Int. Ed.* **2005**, *44*, 6142.
(26) (a) Rapenne, G.; Dietrich-Buchecker, C.; Sauvage, J.-P. *J. Am. Chem. Soc.* **1999**, *121*, 994. (b) Pomeranc, D.; Heitz, V.; Chambron, J.-C.; Sauvage, J.-P. *J. Am. Chem. Soc.* **2001**, *123*, 12215.
(27) (a) Schubert, U. S.; Eschbaumer, C. *Angew. Chem., Int. Ed.* **2002**, *41*, 2892. (b) Constable, E. C.; Thompson, A. M. W. C. *J. Chem. Soc., Dalton Trans.* **1992**, 3467. (c) Hasenknopf, B.; Lehn, J.-M.; Baum, G.; Fenske, D. *Proc. Natl. Acad. Sci. U.S.A.* **1996**, *93*, 1397. (d) Crane, J. D.; Sauvage, J.-P. *New J. Chem.* **1992**, *16*, 649. (e) Hofmeier, H.; Schubert, U. S. *Chem. Soc. Rev.* **2004**, *33*, 373.
(28) (a) Visinescu, D.; Toma, L. M.; Fabelo, O.; Ruiz-Pérez, C.; Lloret, F.; Julve, M. *Polyhedron* **2009**, *28*, 851. (b) Toma, L. M.; Armentano, D.; Munno, G. D.; Sletten, J.; Lloret, F.; Julve, M. *Polyhedron* **2007**, *26*, 5263.
(29) Tait, S. L.; Wang, Y.; Costantini, G.; Lin, N.; Baraldi, A.; Esch, F.; Petaccia, L.; Lizzit, S.; Kern, K. *J. Am. Chem. Soc.* **2008**, *130*, 2108.
(30) Barth, J. V.; Brune, H.; Ertl, G.; Behm, R. J. *Phys. Rev. B* **1990**, *42*, 9307.
(31) (a) Lin, W.-C.; Chang, H.-Y.; Hu, Y.-C.; Lin, Y.-Y.; Hsu, C.-H.; Kuo, C.-C. *Nanotechnology* **2010**, *21*, 6. (b) Glowatzki, H.; Duhm, S.; Braun, K.-F.; Rabe, J. P.; Koch, N. *Phys. Rev. B* **2007**, *76*, 125425.

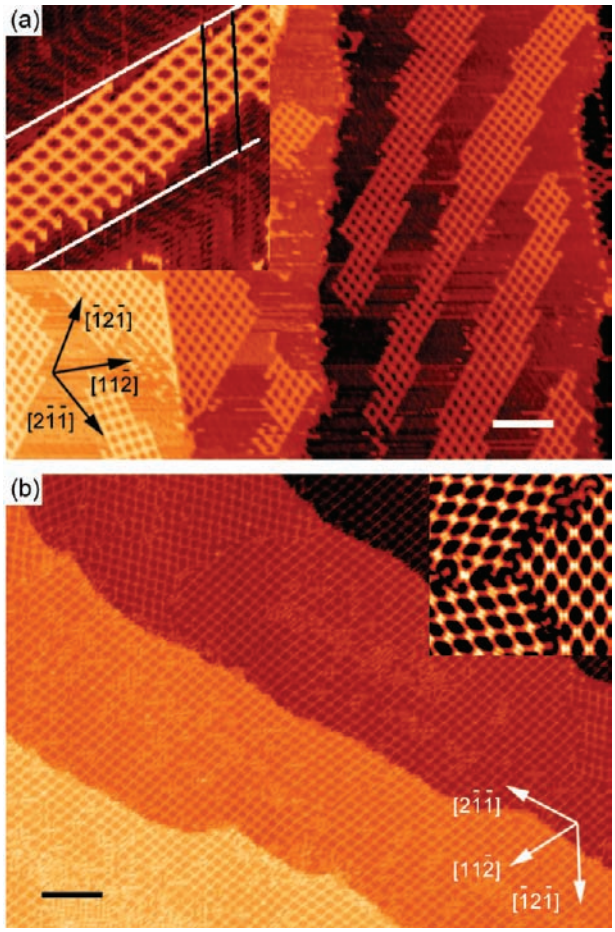


***Figure 2.*** (a) Overview STM topograph of the homogeneous type-I phase at low network coverage, showing the anisotropic growth of network islands (scale bar: 20 nm). The inset (50 nm × 50 nm) shows a network island confined by the herringbone reconstruction domain of the Au(111) surface [data acquisition conditions: $U = -1.4$ V, $I = 0.4$ nA; (inset) $U = -1.4$ V, $I = 0.3$ nA]. (b) Overview STM topograph of the homogeneous type-I phase at high network coverage (scale bar: 20 nm). The inset (30 nm × 30 nm) shows three network domains oriented 120° apart [data acquisition conditions: $U = -1.0$ V, $I = 0.3$ nA; (inset) $U = 1.4$ V, $I = 0.4$ nA].

in Figure 2b. However, the single domains of the network islands do not extend beyond 100 nm in size, suggesting that the templating effect of the Au(111) herringbone reconstruction still plays a role at high network coverage. Domain boundaries between network islands are frequently observed. The inset in Figure 2b, which shows the encounter of three network islands, clearly reveals the 120° angle between the network domains.

The fact that the type-I phase is formed predominantly under these conditions implies that this phase has a relatively low free energy. As discussed previously, the formation energy of the two phases is very close on account of the molecular/atomic adsorption configurations as well as the coordination bonding. One may expect entropy differences to contribute to the free-energy difference. Either the configuration entropy or the local-porosity entropy adapted from Gibbs−Shannon theory has been used to describe the structural complexity of microstructures.[32] Different physical models have been developed to quantify this

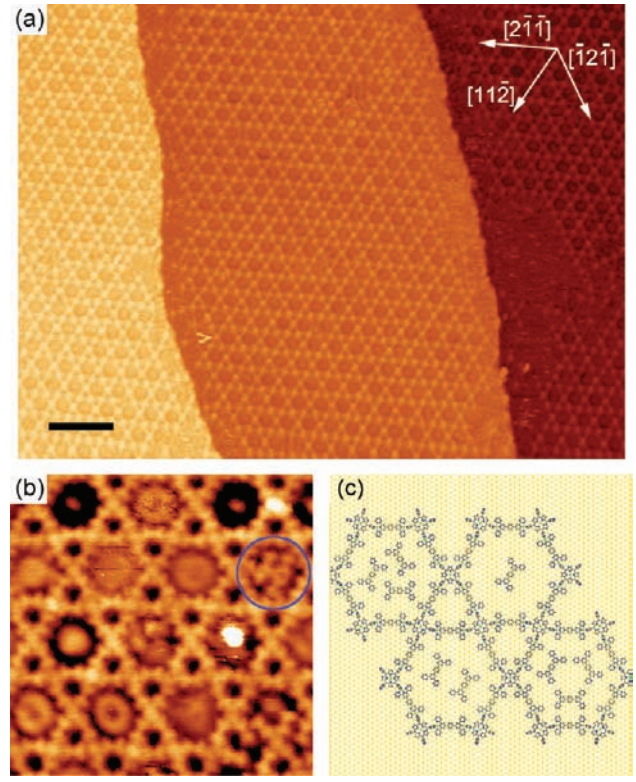


***Figure 3.*** (a) Overview STM topograph of the homogeneous type-II phase (scale bar, 20 nm; data acquisition conditions: $U = 1.4$ V, $I = 0.5$ nA). (b) High-resolution image showing hexagonal voids filled with guest species. The circle marks an inclusion of four molecules of **1** (image size, 25 nm × 25 nm; data acquisition conditions: $U = -1.2$ V, $I = 0.3$ nA). (c) Suggested model of inclusions with one, two, and three molecules of **1**.

property.[33] For example, the maxima and minima in such entropy were shown to correspond to clustering and to periodicity or ordering, respectively.[33a] In our case, the type-II Kagome structure has a higher structural complexity than the type-I rhombus structure. Thus, qualitatively, the former has lower entropy, so its formation is less favored.

Interestingly, we have discovered that the type-II Kagome phase may be formed predominantly by using a guest-inclusion approach. In this approach, a sample of the type-I structure covering the entire surface was prepared first. Next, molecules of compound **1** were deposited onto this sample, and it was annealed at 180 °C, after which the type-II phase appeared to coexist with the type-I phase islands. Further increasing the dosage of compound **1** enlarged the area of the type-II phase and diminished the area of the type-I phase. Eventually, more than 95% of the surface was occupied by the type-II structure at a particular compound **1** dosage. A representative STM overview of a sample dominated by the type-II phase is shown in Figure 3a. As the Kagome structure of the type-II structure has only one orientation with respect to the Au(111) surface lattice, single domains of Kagome structure as large as several hundred nanometers can extend over entire Au(111) terraces, with occasional interruptions by line dislocations.

Close inspection reveals that almost all of the hexagonal voids of the Kagome structure are filled with some guest species.

(32) Shannon, C. E.; Weaver, W. *The Mathematical Theory of Communication*; University of Illinois: Urbana, IL, 1959.

(33) (a) Van Siclen, C. DeW. *Phys. Rev. E* **1997**, *56*, 5211. (b) Andraud, C.; Beghdadi, A.; Haslund, E.; Hilfer, R.; Lafait, J.; Virgin, B. *Physica A* **1997**, *235*, 307. (c) Andraud, C.; Lafait, J. *Phys. Rev. B* **1998**, *57*, 13227.

High-resolution images (e.g., Figure 3b) show that the most frequently observed inclusions are dotlike, bumplike, or donut-like rings or a diffusive "cloud". In some cases, molecules of **1** were resolved as the included species. For example, four molecules of **1** are trapped in the hexagonal void marked by the circle in Figure 3b. This observation suggests that the unresolved inclusions are from molecule(s) of **1** too. It has been found that on surfaces, molecules may rotate or vibrate because of their thermal energy.[34] In confined spaces with high symmetry, thermally moving molecules usually appear as diffusive features with circular symmetry in STM topographs. We propose that the different appearances of the inclusions are produced by thermally moving molecular clusters of **1** having different sizes or different arrangements. As illustrated in Figure 3c, models with one-, two-, and three-molecule inclusions are proposed, corresponding to the dot, bump, donut or "cloudy" appearances, respectively. Other types of inclusions might be from either extra molecules or molecular fragments.

We propose a mechanism for the predominant formation of the Kagome structure. When molecules of **1** are deposited in preformed type-I networks covering the entire surface, they are trapped in the networks' voids as guest species. As the compound **1** dosage is increased, the voids host multiple guest molecules. These guest molecules experience intermolecular repulsion due to the limited void space. At an appropriate annealing temperature, the relatively small rhombic voids are expanded by the included guest molecules, forming Kagome networks whose large voids can accommodate the guest molecules with less intermolecular repulsion. Thus, the predominant formation of the Kagome structure relies on an inclusion effect. Inclusion template growth is a well-known phenomenon in 3D coordination framework synthesis.[11] On liquid−solid interfaces, inclusion-induced phase transitions have been documented as well.[18] Here we have demonstrated that the 2D coordination network of smaller voids can be converted into that of larger voids by inclusion of guest molecules of the proper size.

In order to obtain a thorough picture of the phase transition, we conducted series of sequential-deposition experiments. (It should be noted that we always slightly overdosed Fe to ensure that there were enough Fe atoms to coordinate all of the molecules. Under these conditions, the structure formation was independent of the Fe dosage.) One example is indicated by the kinked red line in Figure 4, which represents a four-step process: (1) a sample with nearly normal stoichiometry at low dosage was prepared; (2) the dosage of **1** was increased by ∼80%; (3) the dosage of **2** was increased by ∼80%; and (4) the dosage of **1** was further increased by ∼30%. An annealing treatment at ∼180 °C was applied after each step, and STM topographs were acquired at every step to determine the network structures. The overall results for all of the trials are summarized as a phase diagram shown in Figure 4, where the dashed line denotes the normal stoichiometry (**1**/**2** = 2:1). Three zones are defined: the pure type-I phase as zone I, the pure type-II phase with inclusion as zone II, and the mixture phase containing both type-I and type-II structures as zone III. In zone I, the networks partially cover the surface while the compound **1** dosage is above its normal stoichiometry value. The extra molecules of

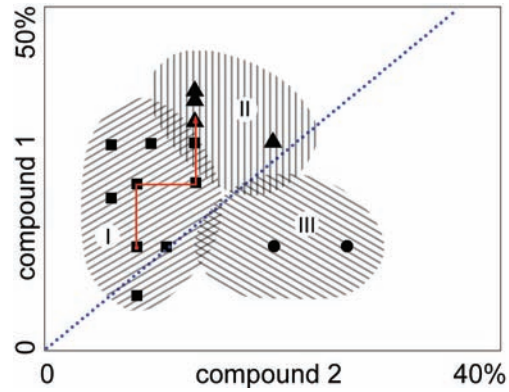


***Figure 4.*** Phase diagram of the polymorphic coordination network structure as a function of the dosages of compounds **1** and **2** (100% corresponds to full surface coverage by molecules). Zones I and II correspond to type-I and filled type-II networks, respectively, and zone III is a mixture phase of the type-I and empty type-II structure. Squares/triangles/circles correspond to experimental data points of type-I, filled type-II and coexistence of type-I and type-II structures. The kinked red line indicates a multistep sequential deposition that resulted in a phase transition from type I to filled type II. The blue dashed line denotes the normal stoichiometry (**1**/**2** = 2:1).

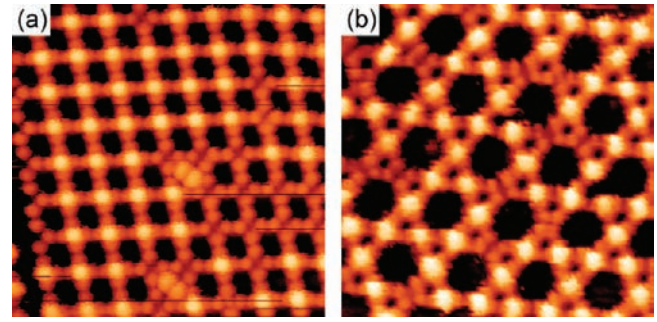


***Figure 5.*** Chemical diversity of molecules of **2** in (a) type-I and (b) type-II networks. Size of each image: 30 nm × 30 nm. Data acquisition conditions: (a) $U = -1.4$ V, $I = 0.6$ nA; (b) $U = -1.4$ V, $I = 0.6$ nA).

**1** exist in a 2D molecular-gas phase,[35] creating noisy STM signals in the surface area outside the network islands. Thus, in zone I, the type-I phase coexists with freely moving molecules of **1**. In zone III, the networks also partially cover the surface while the compound **2** dosage is above its normal stoichiometry value. In this zone, closely packed islands of molecules of **2** are formed (see Figure 1a). In zone II, the networks cover the entire surface, and the extra molecules of **1** are trapped in the hexagonal voids of the Kagome networks. Notably, there are no sharp boundaries between the zones, and mixture structures are present there.

Next, we address the chemical characteristics of the networks. Under certain imaging conditions, molecules of **2** could show two distinctive contrasts in STM topographs, namely, bright bumps or dark depressions, as exemplified in Figure 5. This phenomenon occurred in both phases, and the bright/dark species were distributed randomly in the networks. As it is known that iron atoms are able to metalate free-base porphyrin molecules, which usually give rise to a pronounced STM appearance,[36] we attribute this contrast diversity to metalation of molecules of **2** by Fe. In our experiments, since the condition of the STM tip was unknown, it was impossible to conclude unambiguously

(34) Gimzewski, J. K.; Joachim, C.; Schlittler, R. R.; Langlais, V.; Tang, H.; Johannsen, I. *Science* **1998**, *281*, 531.

(35) (a) Berner, S.; Brunner, M.; Ramoino, L.; Suzuki, H.; Güntherodt, H.-J.; Jung, T. A. *Chem. Phys. Lett.* **2001**, *348*, 175. (b) Wakayama, Y.; Hill, J. P.; Ariga, K. *Surf. Sci.* **2007**, *601*, 3984.

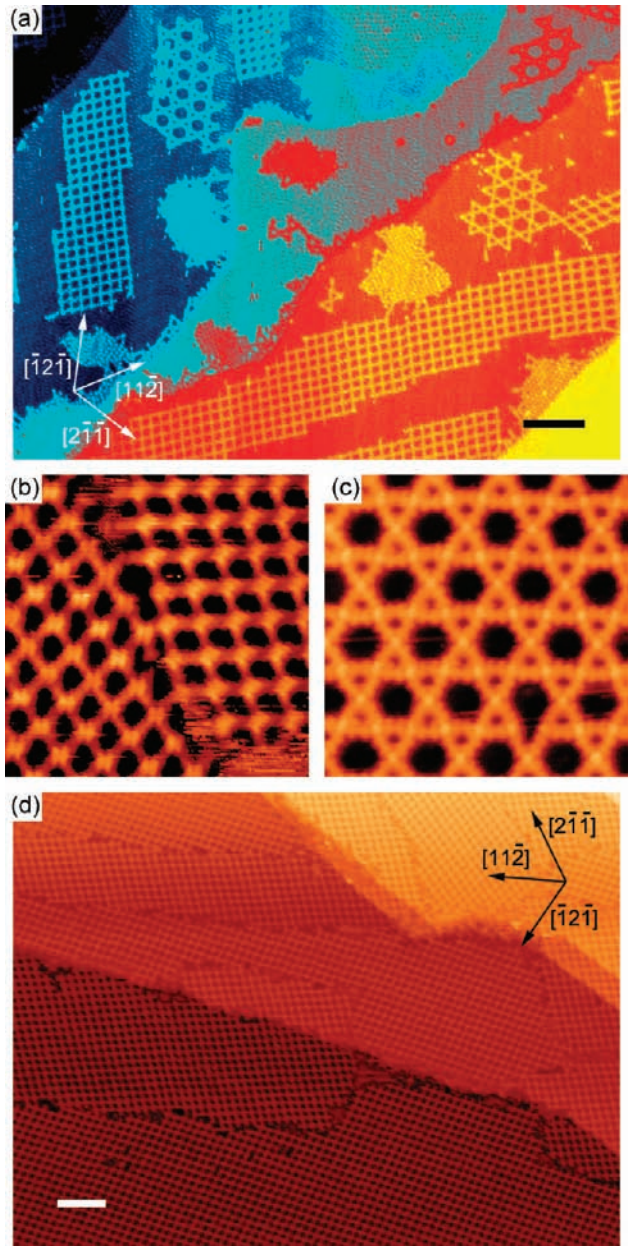


***Figure 6.*** (a) Overview STM topograph of the network structures assembled from **1**, **3**, and Fe, showing type-I and type-II network structures as well as closely packed islands of compound **3** (scale bar, 20 nm; data acquisition conditions: $U = -1.3$ V, $I = 0.5$ nA). (b, c) High-resolution images of the two types of networks showing the homogeneous appearances of compound **3** [size of each image, 30 nm × 30 nm; data acquisition conditions: (b) $U = 1.4$ V, $I = 0.4$ nA; (c) $U = -1.0$ V, $I = 0.6$ nA]. (d) STM topograph showing networks of the homogeneous chemical and structural state (scale bar, 20 nm; data acquisition conditions: $U = 1.7$ V, $I = 0.7$ nA).

which species in our data correspond to metalated porphyrins. Nevertheless, we carried out a series of experiments with varying Fe dosage in order to prepare a phase that would provide us with a homogeneous STM appearance of compound **2**, which is supposed to represent a phase of homogeneous chemical state. All of these trials failed. A likely cause is that Fe atoms participate either in coordination or metalation indiscriminately in the self-assembly processes.

With the aim of preparing networks with homogeneous chemical states, we replaced compound **2** by compound **3**. This compound has been proven to be chemically stable on Au(111) surfaces up to 350 °C.[22] The overview STM topograph in Figure 6a shows structures similar to those in Figure 1a, which shows coexisting type-I and type-II phases. Evidently, the Zn center does not influence the self-assembly processes. In the high-resolution images in Figure 6b,c, all molecules of **3** exhibit an identical appearance, which can be ascribed to the homogenously Zn-metalated compound **3**. Hence, these networks possess porphyrins in a homogeneous chemical state. Finally, we grew networks of a single structure as well as a single chemical state following the protocol outlined in the phase diagram in Figure 4. With appropriate dosages of **1**, **3**, and Fe, type-I networks covering the entire Au surface were formed, as shown in Figure 6d. This phase stands for a bimetallic (Zn and Fe) coordination network of the highest chemical and structural homogeneity.

## Conclusion

In summary, we have investigated the self-assembly of multicomponent 2D coordination networks on a Au(111) surface. The networks consist of two organic molecules as ligands with Fe atoms as coordination metal centers. We have identified two polymorphic types of network structures coexisting on the surface. By tuning the dosage of the constituent compounds, we have realized homogeneous structural phases. We have also demonstrated that inclusion of guest molecules can effectively transform the networks with smaller voids into those with larger voids. Furthermore, we have achieved multicomponent networks with a homogeneous structural and chemical state by using chemically modified ligands. We believe that these results offer an in-depth understanding of complex multicomponent self-assembly, which is of fundamental importance in guiding the bottom-up fabrication of multifunctional nanostructures by supramolecular coordination assembly.

**Acknowledgment.** This work was financially supported by the Hong Kong RGC under Grant 602008.

JA1018578

(36) (a) Shubina, T. E.; Marbach, H.; Flechtner, K.; Kretschmann, A.; Jux, N.; Buchner, F.; Steinrück, H.-P.; Clark, T.; Gottfried, J. M. *J. Am. Chem. Soc.* **2007**, *129*, 9476. (b) Auwärter, W.; Weber-Bargioni, A.; Brink, S.; Riemann, A.; Schiffrin, A.; Ruben, M.; Barth, J. V. *ChemPhysChem* **2007**, *8*, 250. (c) Buchner, F.; Flechtner, K.; Bai, Y.; Zillner, E.; Kellner, I.; Steinrück, H.-P.; Marbach, H.; Gottfried, J. M. *J. Phys. Chem. C* **2008**, *112*, 15458.